Cleaning of Protein−Coated Surfaces Using Nanobubbles: An Investigation Using a Quartz Crystal Microbalance

ARTICLE *in* THE JOURNAL OF PHYSICAL CHEMISTRY C · OCTOBER 2008

Impact Factor: 4.77 · DOI: 10.1021/jp805143c

3 AUTHORS, INCLUDING:

Vincent S J Craig
Australian National University
101 PUBLICATIONS **3,961** CITATIONS

THE JOURNAL OF PHYSICAL CHEMISTRY C

Article

Cleaning of Protein-Coated Surfaces Using Nanobubbles: An Investigation Using a Quartz Crystal Microbalance

Guangming Liu, Zhihua Wu, and Vincent S. J. Craig

J. Phys. Chem. C, **2008**, 112 (43), 16748-16753 • DOI: 10.1021/jp805143c • Publication Date (Web): 08 October 2008

Cleaning of Protein-Coated Surfaces Using Nanobubbles: An Investigation Using a Quartz Crystal Microbalance

Guangming Liu,[†] Zhihua Wu,[‡,§] and Vincent S. J. Craig*[,†]

Department of Applied Mathematics, Research School of Physical Sciences and Engineering, The Australian National University, Canberra, ACT 0200, Australia, State Key Laboratory of Food Science and Technology, Nanchang University, Nanchang, China, and Nanobiology Laboratory, College of Life Science, Shanghai Jiaotong University, Shanghai, China

Received: June 11, 2008; Revised Manuscript Received: July 28, 2008

The use of nanobubbles as cleaning agents to remove bovine serum albumin from the solid−liquid interface has been investigated using a Quartz Crystal Microbalance to both qualitatively follow the production of nanobubbles and to quantify the adsorption to and removal of protein using nanobubbles from both hydrophobic and hydrophilic surfaces. The protein is completely removed from both hydrophobic and hydrophilic surfaces using electrochemically produced nanobubbles after two and four cycles, respectively, of nanobubble production for 10 s periods. The cleaning efficiency compares favorably with treatment for 20 min with a common surfactant, SDS. As nanobubbles are easily produced electrochemically, this process forms the basis of a highly effective, rapid cleaning technique that is environmentally friendly and can be applied to any conducting substrate.

Introduction

Until recently, the proposed existence of nanobubbles at surfaces has been controversial. Theoretically, very small bubbles should rapidly dissolve due to high internal pressure as described by the Laplace equation;[1,2] therefore, the existence of nanobubbles has been disputed. Further, a range of experiments that may be expected to reveal the presence of nanobubbles found no evidence for their existence.[3,4] On the other hand, the evidence for nanobubbles has continued to mount, including direct observations by atomic force microscopy and cryo-SEM imaging.[5−11] The adoption of techniques whereby nanobubbles could be produced under controlled conditions has led to a series of recent publications that have revealed that nanobubbles are indeed stable and that this stability is related to a lower than expected interfacial curvature, due to an anomalously high contact angle.[10,12] The bubble morphology is of spherical caps,[12] and they have been proven spectroscopically to consist of gas.[13] Furthermore, the same solvent exchange technique has been adopted to produce nanolenses of oil drops,[14] providing further evidence that our understanding of the process is valid. Under conditions of mild gas supersaturation such as by solvent exchange, nanobubbles are known to form on hydrophobic surfaces in water.[15] Surface supersaturation and nanobubble production can also be achieved conveniently by electrolysis as employed here.[16]

Cleaning technologies are widely employed and important in a great number of applications. Two approaches are employed: (i) the prevention of adhesion of contaminants by means such as antifouling coatings such as PEG films and (ii) the removal of contaminants following adhesion, which can be achieved chemically, mechanically, and optically.[17,18] Nanobubbles have previously been reported as effective in the prevention of fouling.[19,20] Fouling prevention is simply achieved by a barrier effect whereby the material is prevented from coming into contact with the surface of interest by a layer of nanobubbles. Here we are interested in the removal of material that has already adsorbed to a surface. We anticipate that this approach may be of interest in any system where biomedia lead to fouling, as well as the removal of nonbiological polymers from surfaces.

Materials and Methods

A KSV Quartz Crystal Microbalance (QCM) employing a 5 MHz AT cut quartz crystal with gold electrodes was used to follow the adsorption and desorption of proteins and surfactant as well as the production and removal of nanobubbles. After RF plasma treatment at a power level of 30 W for 60 s, the gold surface of the quartz crystal was rendered hydrophobic by exposure to a 5 mM ethanolic solution of 1-dodecanethiol (AR grade, Aldrich) for a period of 12 h. When a hydrophilic surface was required, the gold electrode surface of the quartz crystal was exposed to a 5 mM ethanolic solution of 11-mercaptoundecanoic acid (AR grade, Aldrich) for a period of 12 h following the same RF plasma treatment as above. Following treatment, the crystal was thoroughly rinsed in ultrapure ethanol and dried under a nitrogen stream. The monolayers were characterized by measurement of the contact angle obtained with pure water using a KSV Cam 200 Contact Angle Goniometer. Modifications were made to the QCM permitting electrolysis to be performed using the gold surface of the quartz crystal as the working electrode, without any change to the mounting of the crystal. This is important as disturbance of the crystal can lead to significant changes in the measured resonant frequency. In an additional experiment, a 5 MHz AT cut quartz crystal with gold electrodes and an overcoat of silicon was employed. The outer layer of the silicon had a thin insulating oxide layer.

Electrochemical treatment was achieved using the gold coated quartz resonator as the cathode and a stainless steel surface as the anode. When a DC voltage (~3.2 V) was applied between the resonator and the stainless steel surface, water was electro-

* To whom correspondence should be addressed. E-mail address: vince.craig@anu.edu.au.
[†] The Australian National University.
[‡] Nanchang University.
[§] Shanghai Jiaotong University.

10.1021/jp805143c CCC: $40.75
Published on Web 10/08/2008

lyzed into molecular hydrogen and oxygen, and the supersaturated hydrogen formed nanobubbles at the liquid−resonator interface. A switch was used to control the time of electrochemical treatment. Typically, the time allowed for electrolysis was 10 s for each cycle.

QCM is commonly employed to follow the adsorption of surfactants, particles, polymers, and proteins to a substrate.[21−26] The change in resonant frequency (Δf) of the crystal can be related to the adsorbed amount (Δm) using the Sauerbrey equation,[27] which is known to perform well for films that behave elastically.

$$\Delta m = -\frac{\rho_q l_q}{f_0}\frac{\Delta f}{n} \quad (1)$$

where f_0 is the fundamental frequency; n is the overtone number; and ρ_q and l_q are the specific density and thickness of the quartz crystal, respectively. In the case of adsorbed proteins, the mass calculated using the Sauerbrey equation, hereafter called the Sauerbrey mass, also includes a contribution due to the mass of entrained water in the film, and therefore adsorbed amounts determined by QCM routinely exceed adsorbed amounts determined by other methods. The degree of solvent coupling can be determined by use of deuterated solvents[28] or comparison with other methods. Changes in conformation of the protein film lead to changes in the degree of solvent coupling and result in changes in the resonant frequency of the crystal. In this study, the solution conditions remained unchanged throughout the experiment so the conformation of the protein is expected to be unchanged. As such, the resonant frequency can be used to quantitatively follow changes in the amount of adsorbed protein.

The resonant frequency is also strongly influenced by the density and viscosity of the solvent in which the crystal is immersed as described by the equation of Kanazawa and Gordon.[29]

$$\Delta f = -n^{0.5} f_0^{1.5} (\eta_l \rho_l / \pi \mu_q \rho_q)^{0.5} \quad (2)$$

where μ_q is the shear modulus of quartz; ρ_q is the density of quartz; and ρ_l and η_l are the density and viscosity of the liquid medium, respectively. For this reason, protein adsorption studies are routinely conducted such that a baseline resonant frequency value is first obtained in the same solvent without protein. Thus, upon exposure to the protein solution, the change in resonant frequency is related only to the protein adsorption and is described by the Sauerbrey equation (i.e., eq 1). The presence of nanobubbles on the surface will alter the resonant frequency, as the effective density and viscosity of the solvent in contact with the crystal are reduced. Additionally, there may be an effect due to a change in hydrodynamic boundary condition.[30−32] Thus an increase in the resonant frequency is attributable to the presence of nanobubbles on the surface, though at this stage we cannot quantitatively determine the nanobubble surface density or morphology. Nonetheless, the presence and removal of nanobubbles can be semiquantitatively followed through changes in the resonant frequency. In the present study, all the results were obtained from the measurements of frequency shifts in the third overtone ($n = 3$) and were conducted at 25 °C. The third overtone is preferred over the fundamental overtone as the resonator is less affected by mechanical forces associated with mounting the resonator, in comparison to the fundamental frequency.

All water used was prefiltered through a coarse wool filter, charcoal filter, and reverse osmosis membrane before a final filtration through a Millipore Gradient system (Memtec) giving a resistivity of 18.2 MΩ cm^{-1}. Phosphate buffer (PB, 10 mM, pH = 7.4) was prepared using potassium phosphate (KH_2PO_4) and sodium phosphate dibasic (Na_2HPO_4). When it was necessary to remove nanobubbles from the surface, the cell was rinsed with degassed phosphate buffer. Degassing was achieved by exposing the buffer to a vacuum (∼1 torr) and mechanical disturbances for at least 2 h before rinsing the cell. The degassed buffer was maintained at low pressure, except when rinsing the cell to ensure it remained degassed. BSA (bovine serum albumin, molecular weight ∼ 66 kDa) was purchased from Aldrich. Sodium dodecyl sulfate (SDS) was purchased from BDH Biochemical and purified by recrystallization from high-purity ethanol prior to use.

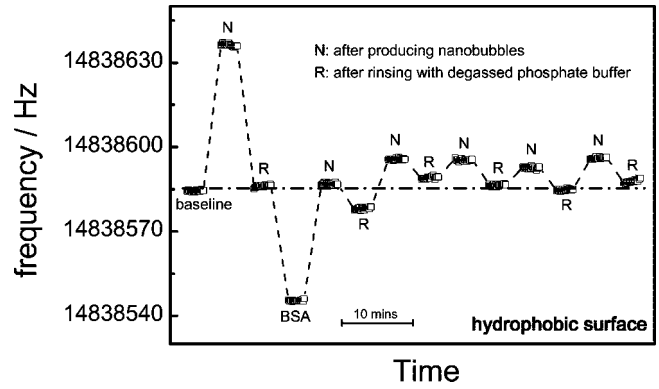

Figure 1. Resonance frequency observed for a series of nanobubble production and removal cycles on a hydrophobic surface. The baseline resonant frequency is obtained for a gold-coated crystal bearing a monolayer of 1-dodecanethiol in phosphate buffer. Before BSA was introduced, nanobubbles were produced and removed, and the baseline signal was recovered. N indicates the resonant frequency measured after 10 s of electrochemical treatment to produce nanobubbles, and R indicates the resonant frequency measured after the removal of such nanobubbles by rinsing four times with degassed phosphate buffer. Subsequently, BSA was introduced, and the resonant frequency was measured again following four rinses with phosphate buffer. Five further cycles of nanobubble production and removal are shown. Note that the data obtained during the rinsing process are very noisy and have been removed from this and subsequent figures for clarity. An example of the raw data indicating the data removed and the data accepted is provided in the Supporting Information. The time scale is indicated by the scale bar.

Results and Discussion

As QCM data are interpreted in terms of changes in the resonant frequency of the Quartz Crystal, it is necessary to adopt a protocol that enables data to be referenced to an appropriate baseline. The baseline used in these studies was the gold substrate coated with the relevant thiol monolayer in phosphate buffer. The baseline resonance frequency varies from experiment to experiment primarily due to differences between quartz resonators, although the mounting of the crystal can also play a role. In the first study, we present a hydrophobic surface that was produced using a monolayer of 1-dodecanethiol (advancing contact angle $\Theta_A = 102°$, receding contact angle $\Theta_R = 95°$). In the second study, a hydrophilic surface was produced using a monolayer of 11-mercaptoundecanoic acid ($\Theta_A = 59°$, $\Theta_R = 39°$). BSA was chosen as a model protein in the present study.

In Figure 1, the baseline refers to the resonant frequency obtained in phosphate buffer with a 1-dodecanethiol monolayer, and this value is shown with a horizontal line at a frequency of ∼ 14 838 585 Hz. Next it was established that electrochemical treatment for 10 s resulted in the production of nanobubbles on the surface, as indicated by an increase of ∼ 51 Hz in the resonant frequency and that these nanobubbles could be removed

by exchange of the buffer with degassed buffer. We note that nanobubbles are more easily produced in the regular buffer solution as opposed to degassed buffer solution. Presumably, this is simply due to differences in the level of gas supersaturation. Upon removal of the nanobubbles, the resonant frequency was ~ 14 838 586 Hz indicating approximately 98% removal of the nanobubbles by the introduction of degassed buffer.

Following this, the surface was exposed to BSA (1 mg mL^{-1}) for a period of 30 min, and then the BSA solution was rinsed four times and replaced with phosphate buffer. The resonant frequency dropped by ~40 Hz to ~14 838 546 Hz. This corresponds to a Sauerbrey mass of ~2.36 mg m^{-2} which is comparable to that expected for a close-packed monolayer of BSA which has a surface excess of 2.5 mg m^{-2}, when the BSA molecule is adsorbed on its longer side that is in the prolate conformation.[19,33] Note that the mass in the present work includes any water entrained in the protein film.

As the rinsing process introduces injection spikes into the data, these data have been removed from the figures in this paper as have the data where the system is equilibrating. An example of the untreated data is provided in the Supporting Information. Nanobubbles were then produced electrochemically for 10 s resulting in an increase in the resonant frequency by ~41 Hz. This change in resonant frequency has two additive contributions, one due to the production of nanobubbles and one due to removal of protein. To determine the change in resonant frequency due to removal of protein, the nanobubbles must first be removed. This is achieved by rinsing with the degassed phosphate buffer and allowing the quantity of BSA remaining on the surface to be determined. In practice, four rinses were employed, and as described above, the data during the rinsing process were subsequently deleted due to the presence of injection spikes. In Figure 1, five cycles of nanobubble production and removal are shown. After only two cycles, it can be seen that the BSA is completely removed from the surface indicating that nanobubbles are highly effective agents for the removal of proteins from hydrophobic surfaces. In a control experiment, it was shown that the electrochemical treatment did not significantly degrade the alkanethiol monolayer. The contact angles before electrochemical treatment were $\Theta_A = 102°$ and $\Theta_R = 95°$ and after treatment were $\Theta_A = 98°$ and $\Theta_R = 90°$, a small reduction. Therefore, the changes in resonant frequency and removal of the protein cannot be attributed to the breakdown of the hydrophobic monolayer. We note that the frequency change initially obtained on the bare thiol surface is far greater than the frequency change obtained during protein removal, even when most of the protein had been removed. The initial production of nanobubbles took place in a buffer solution that had not been degassed, whereas subsequent electrochemical treatments all take place in degassed buffer solutions. In a separate experiment, we have established that the level of dissolved gas in the buffer solution is the cause of this discrepancy (see Supporting Information).

We have also investigated the use of nanobubbles as cleaning agents on comparatively hydrophilic surfaces, using an 11-mecaptoundecanoic acid monolayer. The vast majority of studies have reported that nanobubbles are present on hydrophobic surfaces, and it is generally not thought that they are found on hydrophilic surfaces. In Figure 2, we see that the production of nanobubbles on a hydrophilic surface can be readily achieved electrochemically and followed using the increase in resonant frequency and that the nanobubbles are removed upon introduction of the degassed buffer as observed above. On the hydrophilic surface, the resonant frequency dropped by ~90 Hz upon

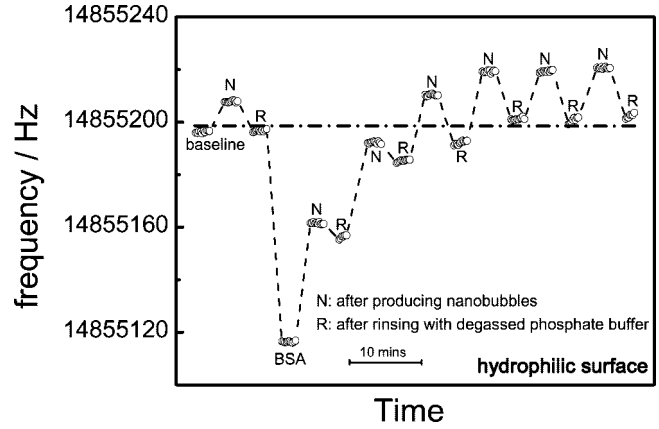

Figure 2. Resonance frequency observed for a series of nanobubble production and removal cycles on a hydrophilic surface. The baseline resonant frequency is obtained for a gold-coated crystal bearing a monolayer of 11-mecaptoundecanoic acid in phosphate buffer. Before BSA was introduced, nanobubbles were produced and removed, and the baseline signal was recovered. N indicates the resonant frequency measured after 10 s of electrochemical treatment to produce nanobubbles, and R indicates the resonant frequency measured after the removal of such nanobubbles by the introduction of degassed phosphate buffer. Subsequently, BSA was introduced, and the resonant frequency was measured. Six further cycles of nanobubble production and removal are shown. The time scale is indicated by the scale bar.

exposure to the BSA solution. This corresponds to a Sauerbrey mass of ~5.31 mg m^{-2}. The greater adsorbed amount on the hydrophilic surface may be due to either a contribution of entrained water or a change in the adsorption of the BSA to an end-on or prolate configuration as seen on HOPG in ethanolic solutions.[20,26] Following the same protocol as above, we present six cycles of nanobubble production and removal. It is evident that nanobubbles remove the protein from the surface completely after four cycles, indicating that nanobubbles are also effective cleaning agents for hydrophilic surfaces. The electrochemical treatment had little effect on the wettability (before, $\Theta_A = 59°$, $\Theta_R = 39°$; after, $\Theta_A = 57°$, $\Theta_R = 43°$). This indicates that the electrochemical treatment had minimal effect on the hydrophilic monolayer. Accordingly, the frequency change indicating removal of BSA from the surface is attributed to nanobubbles rather than the breakdown of the hydrophilic monolayer. As a further check that the nanobubbles rather than the electromagnetic field are responsible for the cleaning process, we have used a quartz crystal resonator coated with silicon and employed the same electrochemical treatment. The outer layer of the silicon has a thin insulating oxide layer which limits the flow of current upon application of a voltage. In this system, we see a very small frequency change and no removal of protein after electrochemical treatment.

In Figure 3, we compare the efficiency of protein removal in the two systems. It can be seen that protein removal by nanobubbles is more efficient on the hydrophobic surface compared to the hydrophilic surface. BSA can be completely removed from the hydrophobic surface after only two cycles, but it requires four cycles to remove BSA completely from the hydrophilic surface. It is known that the conformation of the adsorbed polymer or protein layer can be probed through the relationship between the dissipation change (ΔD) and the frequency change (Δf),[34−36] where the dissipation factor is unitless and is defined by $D = E_{dissipated}/2\pi E_{stored}$, where $E_{disspated}$ is the energy dissipated during one oscillation and E_{stored} is the energy stored in the oscillating system.[37] The change in dissipation reflects the elasticity of the adsorbed layer. A more

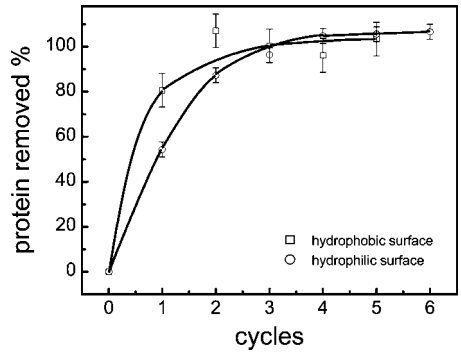

Figure 3. Protein removal versus nanobubble production and removal cycle number, for both hydrophobic and hydrophilic surfaces. The solid lines are provided to guide the eye. The noise level in our frequency measurement is typically less than 1 Hz; however, the main contribution to uncertainty in our measurement is instrumental drift over the time scale of our measurement which is typically 3 Hz or less. Therefore, the error bars correspond to an error of 3 Hz in our measurements.

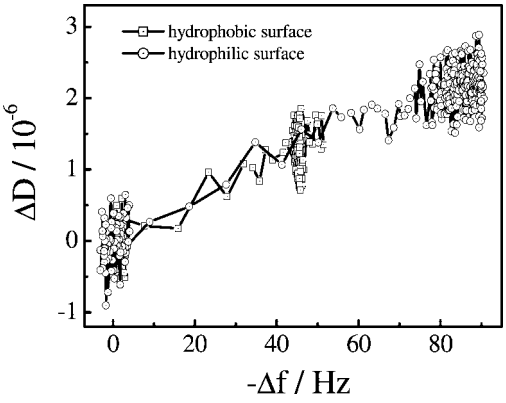

Figure 4. ΔD versus $-\Delta f$ for the adsorption of BSA on hydrophobic and hydrophilic surfaces. The slope of the data for the two systems is comparable indicating that the viscoelasticity of the adsorbed layers is similar, and therefore the conformation of the BSA on the two surfaces is similar. However, the adsorbed mass suggests that the configuration of the molecules differs (see text). The interpretation is that the structure of an individual protein does not vary considerably, but the configuration is such that they lie flat (oblate) on the hydrophobic surface and adopt an end-on (prolate) configuration of the hydrophilic surface.

viscous layer will lead to larger ΔD values for a given change in frequency. In the present study, we find that the relationship between ΔD and Δf for BSA adsorption is the same on a hydrophobic surface and a hydrophilic surface (see Figure 4). This indicates that the viscoelasticity of the BSA films is similar on the two surfaces and suggests that there are no large conformational differences. The greater surface excess obtained for the hydrophilic surfaces is most likely due to an end-on or prolate configuration adopted by the adsorbing proteins rather than a denaturation and increased water entrainment. Therefore, the different cleaning efficiencies between the two surfaces cannot be attributed to large changes in the tertiary structure of the protein. Presumably, the higher efficiency of protein removal on the hydrophobic surface is due to the higher stability of nanobubbles on the surface[12] and the initially lower level of protein coverage. Additionally, the different types of interaction between BSA and the surfaces may lead to different cleaning efficiencies. The adsorption of BSA on the hydrophobic and hydrophilic surfaces is dominated by hydrophobic attraction and hydrogen bonding, respectively.[38] Note that BSA (pI $\sim$ 5.0)[39] and the carboxyl groups (p$K_a \sim$ 4.5)[40] forming the hydrophilic surface are both negatively charged under the conditions employed here; therefore, the electrostatic contribution is

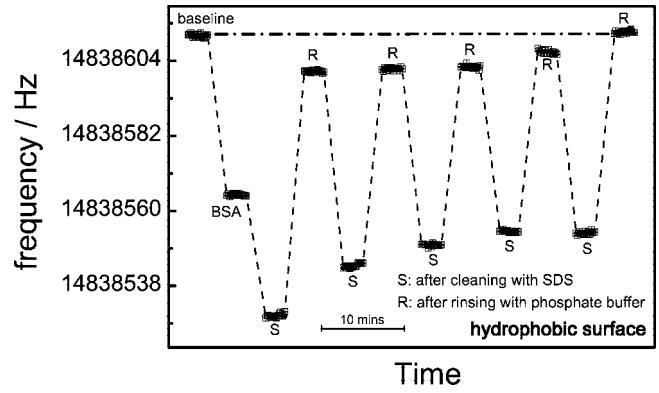

Figure 5. Resonance frequency observed for BSA on a hydrophobic surface during washing cycles using SDS as a detergent. The baseline resonant frequency is obtained for a gold-coated crystal bearing a monolayer of 1-dodecanethiol in phosphate buffer. S indicates the resonant frequency measured after 20 min of cleaning with SDS, and R indicates the resonant frequency measured after rinsing with phosphate buffer. Five cycles of SDS cleaning and phosphate buffer rinses are shown. The time scale is indicated by the scale bar.

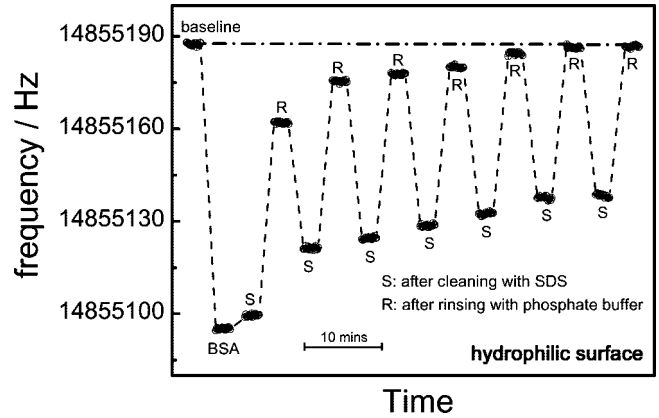

Figure 6. Resonance frequency observed for BSA on a hydrophilic surface during washing cycles using SDS as a detergent. The baseline resonant frequency is obtained for a gold-coated crystal bearing a monolayer of 11-mecaptoundecanoic acid in phosphate buffer. S indicates the resonant frequency measured after 20 min of cleaning with SDS, and R indicates the resonant frequency measured after rinsing with phosphate buffer. Seven cycles of SDS cleaning and phosphate buffer rinse are shown. The time scale is indicated by the scale bar.

expected to oppose adsorption, but one cannot rule out local interactions between the positively charged amino groups and the negatively charged surface.

Surfactants such as SDS are considered as ideal cleaning agents for protein removal from surfaces.[41−43] It was found that there is only a significant desorption of protein from surfaces when the surfactant concentration is larger than the critical micelle concentration (CMC).[43] In the present study, we have investigated the removal of protein from the two surfaces using 17 mM SDS in 10 mM PB solution (above CMC).[44,45] This is shown in Figure 5 for a hydrophobic surface and in Figure 6 for a hydrophilic surface. To investigate cleaning by SDS, the protein was exposed to the SDS containing buffer solution for 20 min before rinsing with the buffer solution. It can be seen that BSA can be completely removed from the hydrophobic surface after five cycles, and it requires six cycles to remove BSA completely from the hydrophilic surface. Note that the introduction of SDS results in a drop in the resonance frequency for the hydrophobic solution but an increase in the resonance frequency for the hydrophilic surface. In both cases, we expect that a small amount of BSA is removed from the surface even

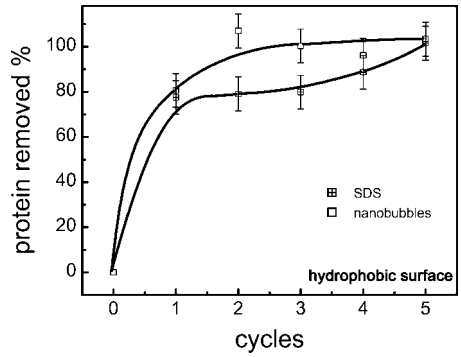

Figure 7. Cleaning efficiency obtained using nanobubbles or SDS on a hydrophobic surface. Each cycle is either 10 s of nanobubble production followed by nanobubble removal by means of exchanging the solvent with degassed phosphate buffer or 20 min exposure to 17 mM SDS in phosphate buffer followed by rinsing with phosphate buffer (without SDS). The solid lines are provided to guide the eye. The noise level in our frequency measurement is typically less than 1 Hz; however, the main contribution to uncertainty in our measurement is instrumental drift over the time scale of our measurement which is typically 3 Hz or less. Therefore, the error bars correspond to an error of 3 Hz in our measurements.

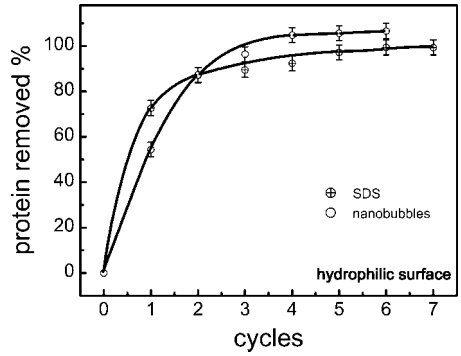

Figure 8. Cleaning efficiency obtained using nanobubbles or SDS on a hydrophilic surface. Each cycle is either 10 s of nanobubble production followed by nanobubble removal by means of exchanging the solvent with degassed phosphate buffer or 20 min exposure to 17 mM SDS in phosphate buffer followed by rinsing with phosphate buffer (without SDS). The solid lines are provided to guide the eye.

before rinsing—this will result in an increase in resonance frequency. However, the SDS will adsorb on the hydrophobic surface through hydrophobic interactions, and the mass of adsorbed SDS results in a decrease in the resonance frequency. As there is a net reduction in frequency on the hydrophobic surface, the influence of SDS adsorption dominates the frequency response. SDS is not adsorbed on the hydrophilic surface, as adsorption is hindered by charge repulsion between the negatively charged headgroup and the negatively charged surface, thus the resonant frequency response is determined by the removal of protein and is seen to increase.

In Figures 7 and 8, we have compared the protein removal efficiency of nanobubbles and SDS for both hydrophobic and hydrophilic surfaces. We find that the protein can be removed completely from both surfaces by either nanobubbles or SDS and that a 10 s nanobubble treatment exhibits a higher efficiency than a 20 min SDS treatment for the hydrophobic surface, and comparable efficiency is obtained for the hydrophilic surface.

Clearly, nanobubbles are highly effective cleaning agents, and they act more quickly than the common surfactant, SDS. Here we have conveniently employed electrochemical methods to produce nanobubbles. We expect that other methods of nanobubble production such as solvent exchange or temperature change may also result in effective cleaning. Further, these methods may be employed even when the surface is nonconducting. Further studies are underway to investigate how the combination of nanobubbles and SDS may be used to improve the cleaning efficiency.

Conclusion

We have investigated the nanobubble facilitated removal of protein from both hydrophobic and hydrophilic surfaces using electrochemically generated nanobubbles, using QCM. The measured changes in resonant frequency indicate that nanobubbles are highly effective cleaning agents for the removal of proteins from surfaces. Additionally, nanobubbles are readily produced on both hydrophobic and hydrophilic surfaces electrochemically, and their effectiveness on the former is superior. In comparison with a 20 min treatment with SDS, a 10 s nanobubble treatment exhibits greater cleaning efficiency on hydrophobic surfaces and a similar efficiency on hydrophilic surfaces. In summary, the present method is an effective, rapid, low cost, environmentally friendly surface cleaning technique suitable for conducting surfaces.

Acknowledgment. V.S.J.C. gratefully acknowledges support from the Australian Research Council.

Supporting Information Available: (1) An example of the raw data (resonant frequency versus time) for the production of nanobubbles and the removal of BSA by nanobubbles from a hydrophobic surface, corresponding to Figure 1. (2) Data showing the change in resonant frequency due to the initial production of nanobubbles in degassed buffer. (3) An investigation of the resonance frequency when a silicon-coated resonator is employed. This material is available free of charge via the Internet at http://pubs.acs.org.

References and Notes

(1) Eriksson, J. C.; Ljunggern, S. *Colloids Surf., A* **1999**, *159*, 159.
(2) Ljunggern, S.; Eriksson, J. C. *Colloids Surf., A* **1997**, *129−130*, 151.
(3) Poynor, A.; Hong, L.; Robinson, I. K.; Granick, S.; Zhang, Z.; Fenter, P. A. *Phys. Rev. Lett.* **2006**, *97*, 266101.
(4) Mezger, M.; Reichert, H.; Schöder, S.; Okasinski, J.; Schröder, H.; Dosch, H.; Palms, D.; Ralston, J.; Honkimäki, V. *Proc. Natl. Acad. Sci. U.S.A.* **2006**, *103*, 18401.
(5) Agrawal, A.; Park, J.; Ryu, D.; Hammond, P.; Russell, T.; McKinley, G. *Nano Lett.* **2005**, *5*, 1751.
(6) Holmberg, M.; Kuhle, A.; Garnaes, J.; Morch, K.; Boisen, A. *Langmuir* **2003**, *19*, 10510.
(7) Ishida, N.; Inoue, T.; Miyahara, M.; Higashitani, K. *Langmuir* **2000**, *16*, 6377.
(8) Otsuka, I.; Yaoita, M.; Higano, M.; Nagashima, S. *Surf. Rev. Lett.* **2003**, *10*, 337.
(9) Simonsen, A.; Hansen, P.; Klosgen, B. *J. Colloid Interface Sci.* **2004**, *273*, 291.
(10) Yang, J. W.; Duan, J. M.; Fornasiero, D.; Ralston, J. *J. Phys. Chem. B* **2003**, *107*, 6139.
(11) Fan, Y. W.; Wang, R. Z. *Adv. Mater.* **2005**, *17*, 2384.
(12) Zhang, X. H.; Maeda, N.; Craig, V. S. J. *Langmuir* **2006**, *22*, 5025.
(13) Zhang, X. H.; Khan, A.; Ducker, W. A. *Phys. Rev. Lett.* **2007**, *98*, 136101.
(14) Zhang, X. H.; Ducker, W. A. *Langmuir* **2007**, *23*, 12478.
(15) Zhang, X. H.; Zhang, X. D.; Sun, J. L.; Zhang, Z. X.; Li, G.; Fang, H. P.; Xiao, X. D.; Zeng, X. C.; Hu, J. *Langmuir* **2007**, *23*, 1778.
(16) Zhang, L. J.; Zhang, Y.; Zhang, X. H.; Li, Z. X.; Shen, G. X.; Ye, M.; Fan, C. H.; Fang, H. P.; Hu, J. *Langmuir* **2006**, *22*, 8109.
(17) Prime, K. L.; Whitesides, G. M. *Science* **1991**, *252*, 1164.
(18) Li, Q. L.; Elimelech, M. *Environ. Sci. Technol.* **2004**, *38*, 4683.
(19) Wu, Z.; Zhang, X. H.; Zhang, X. D.; Li, G.; Sun, J. L.; Zhang, Y.; Li, M. Q.; Hu, J. *Surf. Interface Anal.* **2006**, *38*, 990.
(20) Wu, Z.; Zhang, X. H.; Zhang, X. D.; Sun, J. L.; Dong, Y. M.; Hu, J. *Chin. Sci. Bull.* **2007**, *52*, 1913.

(21) Caruso, F.; Serizawa, T.; Furlong, D. N.; Okahata, Y. *Langmuir* **1995**, *11*, 1546.
(22) Plunkett, M. A.; Claesson, P. M.; Rutland, M. W. *Langmuir* **2002**, *18*, 1274.
(23) Seo, H.; Yoo, M.; Jeon, S. *Langmuir* **2007**, *23*, 1623.
(24) Liu, G. M.; Zhao, J. P.; Sun, Q. Y.; Zhang, G. Z. *J. Phys. Chem. B* **2008**, *112*, 3333.
(25) Liu, G. M.; Zou, S. R.; Fu, L.; Zhang, G. Z. *J. Phys. Chem. B* **2008**, *112*, 4167.
(26) Roach, P.; Farrar, D.; Perry, C. C. *J. Am. Chem. Soc.* **2005**, *127*, 8168.
(27) Sauerbrey, G. *Z. Phys.* **1959**, *155*, 206.
(28) Craig, V. S. J.; Plunkett, M. *J. Colloid Interface Sci.* **2003**, *262*, 126.
(29) Kanazawa, K. Z.; Gordon, J. G., III *Anal. Chem.* **1985**, *57*, 1770.
(30) Ferrante, F.; Kipling, A. L.; Thompson, M. *J. Appl. Phys.* **1994**, *76*, 3448.
(31) Ellis, J. S.; Hayward, G. L. *J. Appl. Phys.* **2003**, *94*, 7856.
(32) Du, B. Y.; Goubaidoulline, I.; Johannsmann, D. *Langmuir* **2004**, *20*, 10617.
(33) Fair, B. D.; Jamieson, A. M. *J. Colloid Interface Sci.* **1980**, *77*, 525.
(34) Liu, G. M.; Yan, L. F.; Chen, X.; Zhang, G. Z. *Polymer* **2006**, *47*, 3157.
(35) Liu, G. M.; Cheng, H.; Yan, L. F.; Zhang, G. Z. *J. Phys. Chem. B* **2005**, *109*, 22603.
(36) Otzen, D. E.; Oliveberg, M.; Höök, F. *Colloids Surf., A* **2003**, *29*, 67.
(37) Rodahl, M.; Höök, F.; Krozer, A.; Kasemo, B.; Breszinsky, P. *Rev. Sci. Instrum.* **1995**, *66*, 3924.
(38) Parks, J. S.; Cistola, D. P.; Small, D. M.; Hamilton, J. A. *J. Biol. Chem.* **1983**, *258*, 9262.
(39) Serefoglou, E.; Oberdisse, J.; Staikos, G. *Biomacromolecules* **2007**, *8*, 1195.
(40) Gebhardt, J. E.; Fuerstenau, D. W. *Colloids Surf.* **1983**, *7*, 221.
(41) Rapoza, R. J.; Horbett, T. A. *J. Colloid Interface Sci.* **1990**, *136*, 480.
(42) Sarkar, D.; Chattoraj, D. K. *J. Colloid Interface Sci.* **1996**, *178*, 606.
(43) Fröberg, J. C.; Blomberg, E.; Claesson, P. M. *Langmuir* **1999**, *15*, 1410.
(44) Fish, W. W. *J. Agric. Food Chem.* **2006**, *54*, 8294.
(45) Gębicka, L.; Didik, J. *Acta Biochim. Pol.* **2005**, *52*, 551.

JP805143C